RESEARCH ARTICLE

WILEY | Journal of Cellular Biochemistry

Effect of 3,6-anhydro-L-galactose on α-melanocyte stimulating hormone-induced melanogenesis in human melanocytes and a skin-equivalent model

Ji Hye Kim[1,2] | Dong Hyun Kim[3] | Kyung Mun Cho[3] | Kyoung Heon Kim[3] | Nam Joo Kang[1] 🟢

[1]Department of Food Science and Biotechnology, Kyungpook National University, Daegu 41566, Republic of Korea

[2]Korean Medicine Application Center, Korea Institute of Oriental Medicine, Daegu, Republic of Korea

[3]Department of Biotechnology, Graduate School, Korea University, Seoul, Republic of Korea

Correspondence
Kyoung Heon Kim, Department of Biotechnology, Graduate School, Korea University, Seoul 02841, Republic of Korea.
Email: khekim@korea.ac.kr
Nam Joo Kang, Department of Food Science and Biotechnology, Kyungpook National University, Daegu 41566, Republic of Korea.
Email: njkang@knu.ac.kr

Abstract

3,6-Anhydro-L-galactose (L-AHG) is a bioactive sugar that is a major component of agarose. Recently, L-AHG was reported to have anti-melanogenic potential in human epidermal melanocytes (HEMs) and B16F10 melanoma cells; however, its underlying molecular mechanisms remain unknown. At noncytotoxic concentrations, L-AHG has been shown to inhibit alpha-melanocyte-stimulating hormone-induced melanin synthesis in various cell models, including HEMs, melan-a cells, and B16F10 cells. Although L-AHG did not inhibit tyrosinase activity in vitro, reverse transcription-polymerase chain reaction results demonstrated that the anti-melanogenic effect of L-AHG was mediated by transcriptional repression of melanogenesis-related genes, including tyrosinase, tyrosinase-related protein-1 (TRP-1), tyrosinase-related protein-2 (TRP-2), and microphthalmia-associated transcription factor (MITF) in HEMs. Western blot analysis showed that L-AHG effectively attenuated α-melanocyte-stimulating hormone-induced melanogenic proteins by inhibiting cyclic adenosine monophosphate/cyclic adenosine monophosphate–dependent protein kinase, mitogen-activated protein kinase, and Akt signaling pathways in HEMs. Topical application of L-AHG significantly ameliorated melanin production in a 3D pigmented human skin model. Collectively, these results suggest that L-AHG could be utilized as novel cosmetic compounds with skin-whitening efficacy.

KEYWORDS
3,6-anhydro-L-galactose (L-AHG), alpha-melanocyte-stimulating hormone (α-MSH), human melanocytes, human skin equivalent, melanogenesis

1 | INTRODUCTION

Melanogenesis is a complex process of melanin production in melanocytes.[1] Melanin pigments play an important role in the determination of skin color and protection of the skin from ultraviolet (UV).[2,3] However, abnormal accumulation of melanin leads to skin hyperpigmentary disorders, such as freckles, melasma, and age spots.[3] Skin pigmentation defects are associated with several regulatory factors,

such as intrinsic or extrinsic factors, which are primarily regulated by UV. In response to UV, various stimulators, such as alpha-melanocyte-stimulating hormone (α-MSH), are induced from keratinocytes and subsequently α-MSH upregulates melanin synthesis in melanocytes.

α-MSH stimulates melanocortin 1 receptor (MC1R), which subsequently activates adenylate cyclases.[4-6] Activated adenylate cyclases converts ATP into cyclic adenosine monophosphate (cAMP) in melanocytes.[7,8] Intracellular cAMP upregulates transcriptional factors, such as microphthalmia-associated transcription factor (MITF) and cAMP response element-binding protein (CREB), through diverse signaling pathways.[9,10] Protein kinase A (PKA) is the main signaling pathway known to have cellular cAMP-dependent activity. The inactive form of PKA is a complex of a regulatory subunit dimer (PKA_{RI}, PKA_{RII}) and 2 catalytic subunits (PKA-$_{Cat).}$[11] Two cAMP molecules bind to each regulatory subunit of PKA; afterwards, the catalytic subunits are separated and phosphorylate PKA substrates, including the Ser-133 residue of CREB.[11] Phosphorylation of CREB induces the expression of MITF, tyrosinase, and tyrosinase-related proteins (TRPs), leading to melanogenesis.[4,7]

Mitogen-activated protein kinases (MAPK), including p38 MAPK and c-Jun N-terminal kinase (JNK) signaling pathways, are involved in melanocyte differentiation in response to various stress factors, such as UV and heat.[12,13] Moreover, the relationship between MC1R and p38 signaling pathways has been identified in human melanocytes and melanoma cells.[13,14] Stimulation of MC1R by α-MSH triggers cAMP and p38, which leads to the activation of CREB and MITF.[13,14] As well as the p38 signal pathway, elevation of intracellular cAMP activates the extracellular signal-regulated kinase (ERK) signaling pathway in murine melanocytes and melanoma cells.[8,10,11] Phosphorylation of MITF on serine 73 and serine 409 by ERK and ribosomal s6 kinase (RSK)-1, respectively, promotes not only proteosomal degradation but also increased transcriptional activity of MITF.[15-18]

Phosphatidylinositol 3-kinase (PI3K)/Akt have been known to negatively modulate MITF expression through a PKA-independent mechanism.[19,20] cAMP inhibits PI3K and Akt, and promotes the activation of GSK3β by phosphorylating MITF on serine 298.[20,21] In addition, it is suggested that an increased level of cAMP results in the phosphorylation and activation of MITF via inhibition of PI3K/Akt/mammalian target of rapamycin (mTOR)/p70S6Kinase (p70S6K)/glycogen synthase kinase 3 beta (GSK3beta) in melanocytes and melanoma cells.[22,23] Consequently, the activation of GSK3β facilitates MITF binding to the M-box of the tyrosinase promoter, leading to the stimulation of tyrosinase expression.[16,24]

The general approach for the development of anti-melanogenic agents has focused on direct targeting of the components involved in melanin synthesis, such as tyrosinase.[25,26] However, an alternative strategy has been suggested where inhibitors of melanogenesis-related signaling pathways may have sufficient effectiveness and fewer side effects.[26,27] Therefore, suppression of the intracellular melanogenesis signaling pathway may be an effective strategy for the prevention of skin hyperpigmentation.[26,27]

Seaweeds (marine macroalgae) have been considered a promising cosmeceutical material for new melanogenesis inhibitors due to their skin-whitening potential.[28-30] This biological efficacy of marine macroalgae is considered to result from their macroalgae-derived sugars.[28,30,31] According to a recent study, sugars and sugar-related derivatives have been suggested as anti-melanogenic agents with minimal side effects.[26] Sugars are broadly utilized in cosmetic products because of their moisturizing effects and relatively low cytotoxicity.[26] Previously, 3,6-anhydro-L-galactose (L-AHG; Figure 1A) was identified as the key monomeric sugar of red macroalgae with remarkable anti-melanogenic effects in HEMs and B16F10 melanoma cells by our group.[32-34] However, the underlying molecular mechanism of L-AHG has not been fully understood. Here, we report that L-AHG attenuates α-MSH-induced melanogenesis in human melanocytes and a 3-dimensional (3D) pigmented skin model via suppression of cAMP/PKA, MAPK, and Akt signaling pathways.

2 | MATERIALS AND METHODS

2.1 | Materials

Medium 254 and human melanocyte growth supplement were purchased from Cascade Biologics (Portland, OR). Dulbecco modified Eagle medium, penicillin-streptomycin and 0.5% trypsin-ethylene diamine tetra acetic acid were obtained from GIBCO Invitrogen (Auckland, NZ). The primary and secondary antibodies used in this study were purchased from Santa Cruz Biotech (Santa Cruz, CA), Cell Signaling Technology (Danver, MA), or BD Biosciences (San Jose, CA). Chemiluminescence detection kits were purchased from GE Healthcare (Piscataway, NJ). All other chemicals, including α-MSH, were purchased from Sigma-Aldrich (St Louis, MO).

2.2 | Production of L-AHG from agarose

To produce L-AHG in this study, previously used methods were used after a slight modification.[34-36] Briefly, agarose was sequentially degraded using 3 enzymes in the order of
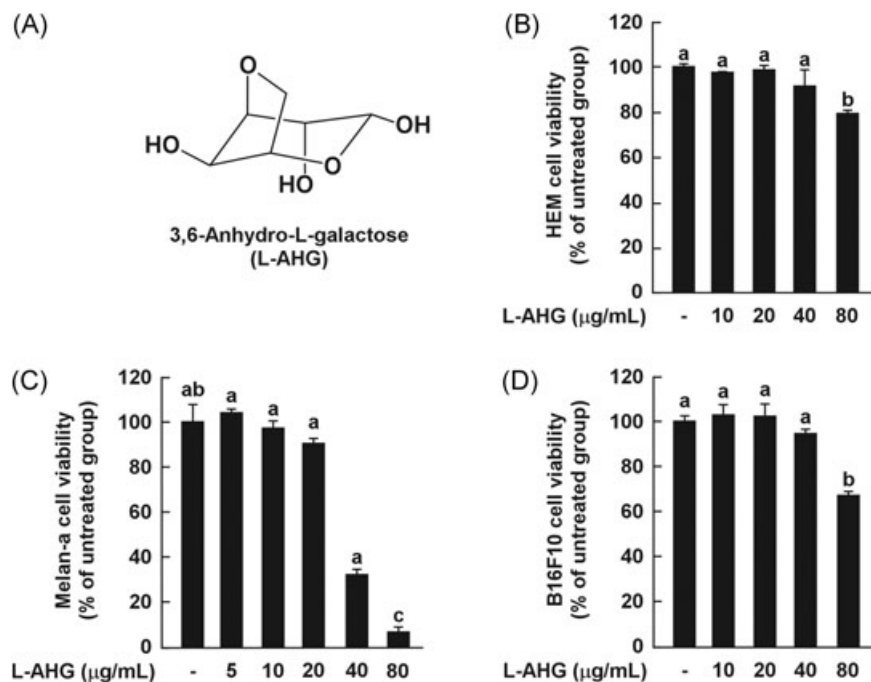
FIGURE 1 Effects of L-AHG on cell viability in various melanin-producing cells. (A) The chemical structures of 3,6-anhydro-L-galactose (L-AHG). Effects of L-AHG on cell viability in various melanocytes, including HEMs (B), melan-a cells (C), and B16F10 cells (D). Cell viability was measured by the MTT assay as described in the Materials and Methods. The results are expressed as the relative percentage of the untreated group. All data (n = 3) represent the mean values ± SD. Means with letters (a-c) in a graph are significantly different from each other at $P < .05$. HEMs, human epidermal melanocytes; SD, standard deviation

Aga16B (an endo-type β-agarase), Aga50D (an exo-type β-agarase), and SdNABH (an α-neoagarobiose hydrolase). These enzymes all originated from Saccharophagus degradans 2-40[T], and their genes were cloned and expressed in Escherichia coli BL21 (DE3).[34-36] In the first enzymatic reaction step, 1% (w/v) agarose was hydrolyzed mainly into neoagarohexaose and neoagarotetraose using 8 mg of Aga16B at 45°C for 1 hour in 100 mL of 20 mM Tris-HCl buffer (pH 7.0). This reaction product was further hydrolyzed into neoagarobiose using 20 mg of Aga50D at 30°C for 2 hours in 20 mM of Tris-HCl buffer (pH 7.0). Finally, to produce L-AHG and D-galactose, the reaction product containing mainly neoagarobiose was added with 2.5 mg of SdNABH, and the enzymatic reaction was performed under the same conditions as those for the reaction with Aga50D.

After all the enzymatic reactions were completed, the reaction products were concentrated using a rotary vacuum evaporator (Eyela, Tokyo, Japan) at 40°C for 2 hours. Purification of L-AHG from the reaction mixtures was performed by silica gel chromatography. A column (I.D. 4 × 100 cm) was packed by silica gel 60 (70-230 mesh ASTM; Merck, Darmstadt, Germany) with methylene chloride. To stabilize the silica gel packing, a mobile phase (methylene chloride/methanol/H_2O = 78:20:2, v/v/v) was passed through the

packed column for 10 minutes. The concentrated enzymatic reaction product was mixed with Celite 545 (Yakuri, Tokyo, Japan) and directly loaded onto the top of the column. The loaded sample was eluted with the mobile phase, and only the fractions containing L-AHG without D-galactose were collected. The collected fractions were dried using a rotary vacuum evaporator at 35°C for 2 hours to remove the mobile phase. L-AHG was dried using a freeze dryer (ilShin Lab Co Ltd, South Korea) and stored at −20°C until further use.

2.3 | Structural analyses of L-AHG

To verify whether the final product from agarose was L-AHG, L-AHG produced and purified in this study was analyzed by 1H-13C nuclear magnetic resonance (NMR) spectroscopy and polarimetry. For the NMR spectroscopy, 2 mg of L-AHG of this study was dried in a centrifugal vacuum concentrator at 30°C for 6 hours and dissolved in D_2O. NMR spectroscopy was performed using a Bruker Avance II 900 MHz NMR spectrometer equipped with a cryoprobe (Bruker, Billerica, MA). The chemical shifts of L-AHG were referenced to 3-(trimethylsilyl)-propionic-2,2,3,3-d4 acid and its chemical structure was verified by comparing the 1H- and 13C-chemical

shifts of L-AHG measured in this study with those of AHG[37] and agarobiose (4-O-(D-galactosyl)-3,6-anhydro-L-galactopyranose)[38] in the literature.

To confirm that the AHG produced in this study has the L-form, the specific rotation of L-AHG was measured using a polarimeter and compared with that of D-AHG and the literature value of L-AHG. Four milligrams of L-AHG produced and purified in this study was dissolved in 2 mL of dH_2O and left at room temperature overnight. The polarimetry of L-AHG was measured with a JASCO P-2000 (JASCO, Easton, MD). The specific rotation was calculated as $= \alpha/lc$, where α is the observed optical rotation (°), l is the length of a sample tube (dm), and c is the solution concentration (g/mL). The specific rotation value of L-AHG was compared with that of D-AHG at 0.3% (w/v) in dH_2O as well as the literature value of L-AHG.[39]

2.4 | Cell culture

Human epidermal melanocytes (HEMs) derived from moderately pigmented neonatal foreskins (HEMs) were purchased from Cascade Biologics. HEMs were cultured in Medium 254 supplemented with human melanocyte growth supplement at 37°C in a humidified atmosphere with 5% CO_2. The murine melanoma cell line B16F10 was obtained from the Korean Cell Line Bank (Seoul, Korea) and cultured in Dulbecco modified Eagle medium supplemented with 10% fetal bovine serum and 1% penicillin/streptomycin at 37°C in a humidified atmosphere with 5% CO_2. Murine melan-a cells, an immortal line of pigmented melanocytes, has been derived from normal epidermal melanoblasts from 18-day-old embryos of inbred C57BL/6J (black, a/a) mice.[40,41] Melan-a cells were kind gift from Prof Dorothy C. Bennett (St. George's Hospital Medical School, London, UK). This cell line was cultured in Roswell Park Memorial Institute (RPMI) 1640 supplemented with 10% fetal bovine serum, 1% penicillin/streptomycin, and 200 nM of 12-O-tetradecanoylphorbol-13-acetate (TPA) at 37°C in a humidified atmosphere containing 10% CO_2.

2.5 | Cell viability

Cell viability was measured using a 3-(4,5-dimethylthiazol-2-yl)-2,5-diphenyltetrazolium bromide (MTT) assay. HEMs and B16F10 cells were cultured in 96-well plates at a density of 1×10^4 cells/well and were incubated in complete culture medium at 37°C in a 5% CO_2 atmosphere. Melan-a cells were cultured in 96-well plates at a density of 1×10^4 cells/well and incubated in complete culture medium at 37°C in a 10% CO_2 atmosphere. After 1 day, the cells were treated with different dosages of L-AHG. After incubation for 3 days, 20 mL of MTT solution was treated for 2 hours at 37°C. The medium was removed and the remaining formazan crystals in the cells were dissolved by dimethyl sulfoxide (DMSO). A microplate reader (Sunrise-Basic Tecan, Tecan Austria GmbH 5082 Groding, Austria) was used to measure the color density at 570 nm.

2.6 | In vitro tyrosinase activity assay

Tyrosinase-inhibitory activity was determined using a method described previously, with minor modifications.[32,42] In a cell-free system, mushroom tyrosinase were used and in a cell model system, cell lysates of HEMs, melan-a, and B16F10 cells were used. Briefly, every reaction contained 50 µL of 0.1 M potassium phosphate buffer (pH 6.8) in a 96-well plate. Next, 5 µL of purified mushroom tyrosinase (Sigma; 2×10^3 units/mL in buffer) or cell extracts and 40 µL of water were added. Test samples (5 µL) were added and the plates were shaken at 25°C for 10 minutes. Next, 50 µL of L-tyrosine solution (0.3 mg/mL in buffer) was added to each well and incubated at 25°C for a few minutes. The formation of dihydroxyphenylalanine (DOPA) was monitored by measuring absorbance at 475 nm using a microplate reader. The % inhibition was calculated using the formula $[(A - B)/A] \times 100$.

2.7 | Measurement of melanin levels

Melanin levels were measured using a method described previously, with slight modifications.[43,44] Briefly, HEMs, B16F10, or melan-a cells (8×10^3 cells/2 mL of complete medium) were seeded into each well of a 6-well plate. After 24 hours, HEMs and B16F10 cells were pretreated with samples (arbutin or L-AHG) at the indicated concentrations for 1 hours before being exposed to α-MSH (100 nM) for the indicated time. Melan-a cells were treated with each sample (arbutin or L-AHG) for 3 days. Then, melanin levels were determined by measuring the absorbance at 495 nm using a microplate reader.

2.8 | Western blot analysis

Cells (1×10^4 cell/mL) were cultured in a 10 cm dish for 24 hours and then treated with L-AHG for 1 hour before being exposed to α-MSH (100 nM) at the indicated times. Protein preparation and Western blot were performed as previously reported.[33] The cells were scraped in a lysis buffer (10 mM Tris [pH 7.5],

150 mM NaCl, 5 mM ethylene diamine tetra acetic acid, 1% Triton X-100, 1 mM dithiothreitol, 0.1 mM phenylmethylsulfonyl fluoride, 10% glycerol, and protease inhibitor cocktail tablet), incubated on ice for 20 minutes, and then centrifuged at 14 000 rpm for 10 minutes. The protein concentrations were measured using a dye-binding protein assay kit purchased from Bio-Rad Laboratories (Hercules, CA) as described by the manufacturer. The proteins were separated by electrophoresis in a 10% sodium dodecyl sulfate-polyacrylamide gel and transferred to a polyvinylidene fluoride membrane from Millipore (Billerica, MA). The membrane was blocked with 5% skim milk for 1 hour 30 minutes and then incubated with the specific primary antibody at 4°C overnight. After hybridization with the secondary antibody, protein bands were visualized using a chemiluminescence detection kit from GE Healthcare Life Sicences Co (Buckinghamshire, UK). Statistical analysis of all western blots is presented in the supplementary data.

2.9 | cAMP immunoassay

The effects of L-AHG on the intracellular cAMP levels were measured using a cAMP immunoassay kit from R&D Systems (Minneapolis, MN), with slight modifications.[45] Briefly, HEMs were cultured in a 10 cm dish for 24 hours. Cells were treated with L-AHG (10 or 20 μM) for 1 hour before being exposed to α-MSH (100 nM) for 15 minutes. Next, the supernatants were prepared and analyzed to measure cAMP levels according to the manufacturer's protocol.

2.10 | Semiquantitative reverse transcription-polymerase chain reaction

For total RNA extraction, HEMs were treated with L-AHG for 1 hour before being exposed to α-MSH (100 nM). After 24 hours, total RNA was prepared using an RNeasy kit (Qiagen, Valencia, CA). Purified total RNA 1 mg was reverse-transcribed with oligo-dT primers using a PrimeScript First Strand complementary DNA (cDNA) Synthesis Kit (TaKaRa Bio Inc, Japan). Amplification consisted of 23-30 cycles: denaturation at 95°C for 45 seconds, annealing at 50°C (glyceraldehyde 3-phosphate dehydrogenase [GAPDH]), 65.8°C (tyrosinase, TRP-1, TPR-2) or 61.2°C (MITF) for 45 seconds, and extension at 72°C for 45 seconds, followed by a final 10 minutes extension at 72°C. Polymerase chain reaction (PCR) was performed using a C1000 Touch™ Thermal Cycler (Bio-Rad Laboratories) in a reaction mixture (50 mL) containing EmeraldAmp GT PCR master mix (TaKaRa,

Shiga, Japan), 60 ng of cDNA, and 0.2 mM of each primer (Macrogen, Seoul, Korea). cDNA was probed with the following primers as previously reported:[46] GAPDH (GenBank accession number: NM_002046, 635 base pairs [bp]) forward 5′-ATGTTCCAATATGATTC CAC-3′, reverse 5′-TCATCATATTTGGCAGG TTT-3′; tyrosinase (NM_000372, 812 bp) forward 5′-TTGGCAT AGACTCTTCTTGTTGCGG-3′, reverse 5′-CAAGGAGC CATGACCAGATCCG-3′; TRP-1 (NM_000550, 1027 bp) forward 5′-TGGCAAAGCGCACAACTCACCC-3′, reverse 5′-AGTGCAACCAGTAACAAAGCGCC-3′; TRP-2 (D17547, 1017 bp) forward 5′-TGTGGAGACTGCAAGTT TGGC-3′, reverse 5′-GAGTTCTTCATT AGTCACTGG AGGG-3′; for MITF-M, the forward primer was selected in the 5′ noncoding region of exon 1 M known to be specifically different from the other MITF isoforms[46] (NM_000248, 962 bp) 5′-ACCGTCCTCCACTGG ATTG GT-3′, reverse 5′-GGAGAGCAGAGACCCGTGGAT-3′. GAPDH was used as a control and variations in the messenger RNA concentration were normalized to GAPDH using Image J program.

2.11 | 3D pigmented human skin model

3D pigmented human skin modeld (Neoderm-ME) were purchased from Tegoscience Co (Seoul, Korea). Samples (arbutin and L-AHG) were applied topically on the surface of a reconstructed pigmented human epidermis model. After 2 days, the MTT assay, the melanin content assay, and Fontana-Masson (F/M) staining were performed for the quantification of melanin levels as described.

2.12 | F/M staining

To visualize intracellular melanin accumulation, F/M staining was performed with a slight modification.[42] 3D human skin-equivalent blocks were fixed with 10% neutral-buffered formalin and embedded in paraffin. The paraffin blocks (3 μm thickness) were sectioned and transferred onto slides. After deparaffinization, the sections were stained with the F/M staining kit from American Master*Tech Scientific, Inc (Lodi, CA) according to the manufacturer's instructions. After dehydration and washing, the sections were observed at 400× magnification using a Nikon phase-contrast microscope (Tokyo, Japan). The images were analyzed using NIS-Elements software and Image J program.

2.13 | Statistical analysis

Experiments were conducted in triplicate and data were expressed as mean ± standard deviation. One-way analysis

of variance was used for single statistical comparisons with IBM SPSS Statistics Version 23.0 (IBM Co, Armonk, NY). In all analyses, a probability value of $P < .05$ was used as the criterion for statistical significance.

3 | RESULTS

3.1 | Effect of L-AHG on cell viability in various melanocytes

To examine the noncytotoxic concentration of L-AHG, the MTT assay was performed in various melanocytes, including HEMs, melan-a cells, and B16F10 cells (Figure 1). L-AHG was not cytotoxic at 10-40 μg/mL in HEMs (Figure 1B) and B16F10 cells (Figure 1D). In melan-a cells, an immortal line of pigmented and murine melanocytes,

L-AHG did not affect cell viability at 5-20 μg/mL (Figure 1C). On the basis of these results, L-AHG concentrations were set up as indicated in the subsequent experiments.

3.2 | Effect of L-AHG on α-MSH-induced melanin production in human melanocytes

To investigate whether L-AHG inhibits α-MSH-induced melanin production in various melanocytes, melanin levels were measured using the melanin content assay (Figure 2). As a positive control, arbutin was used, which is a well-known skin-whitening agent. At noncytotoxic concentrations, L-AHG significantly inhibited the α-MSH-induced melanin production in HEMs and
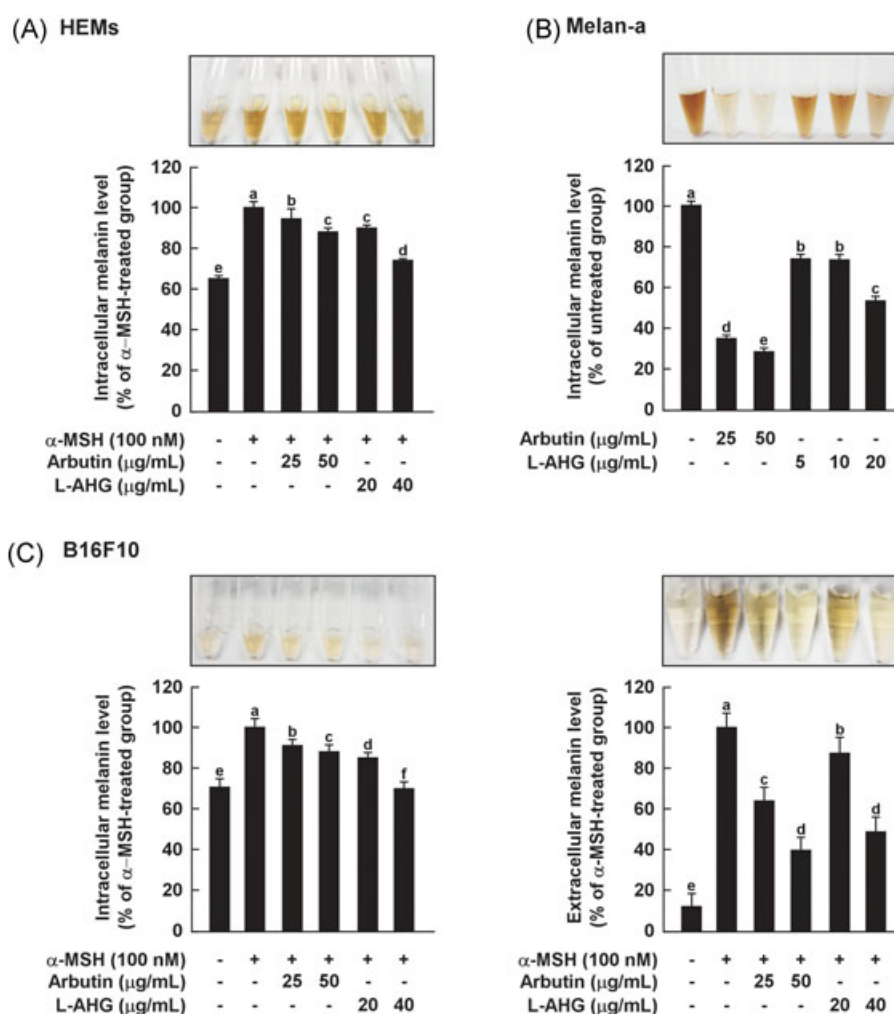

FIGURE 2 Effects of L-AHG on melanin production in various melanin-producing cells, including HEMs. (A), melan-a cells (B) and B16F10 cells (C). The cells were pretreated with samples at the indicated concentrations for 1 hour before being exposed to α-MSH (100 nM) for the indicated times. The melanin levels were determined as described in the Materials and Methods. All data (n = 3) represent the mean values ± SD. Means with letters (a-f) in a graph are significantly different from each other at $P < .05$. α-MSH, alpha-melanocyte-stimulating hormone; HEMs, human epidermal melanocytes; L-AHG, 3,6-anhydro-L-galactose; SD, standard deviation

B16F10 cells (Figure 2A,C). Moreover, L-AHG decreased melanin production in melan-a cells (Figure 2B). These results indicate that L-AHG exerts the anti-melanogenic effect by suppressing melanin synthesis in human and murine melanocytes.

3.3 | Effects of L-AHG on tyrosinase activity in vitro

Tyrosinase is a rate-limiting enzyme that catalyzes L-tyrosine into dopaquinone, resulting in melanin production.[1] To screen tyrosinase inhibitors, mushroom tyrosinase is often used as a substitute for human tyrosinase because it is commercially available in a purified form.[3,42] Therefore, the effect of L-AHG on mushroom tyrosinase activity was examined using L-tyrosine as a substrate. As a positive control, arbutin or kojic acid was used, which are well-known tyrosinase inhibitors. As shown in Figure 3, L-AHG did not inhibit tyrosinase oxidative activity up to 80 μg/mL because

mushroom tyrosinase and mammalian tyrosinase have slightly different amino acid sequences.[47-49] In addition, some compounds that are active against mushroom tyrosinase did not show comparable results with mammalian tyrosinase.[50-52] Therefore, the effect of L-AHG on cellular tyrosinase activity was further investigated using each cell lysate. However, consistent with the above result, L-AHG did not inhibit cellular tyrosinase oxidative activity (Figure 3B-D). These results suggest that the anti-melanogenic effect of L-AHG was not mediated by direct inhibition of tyrosinase activity.

3.4 | Effect of L-AHG on α-MSH-induced melanogenic protein expression in human melanocytes

Melanogenesis is known to be modulated by melanogenic enzymes, including tyrosinase, TRP-1 and TRP-2.[1,8,9] In response to α-MSH treatment, upregulation of
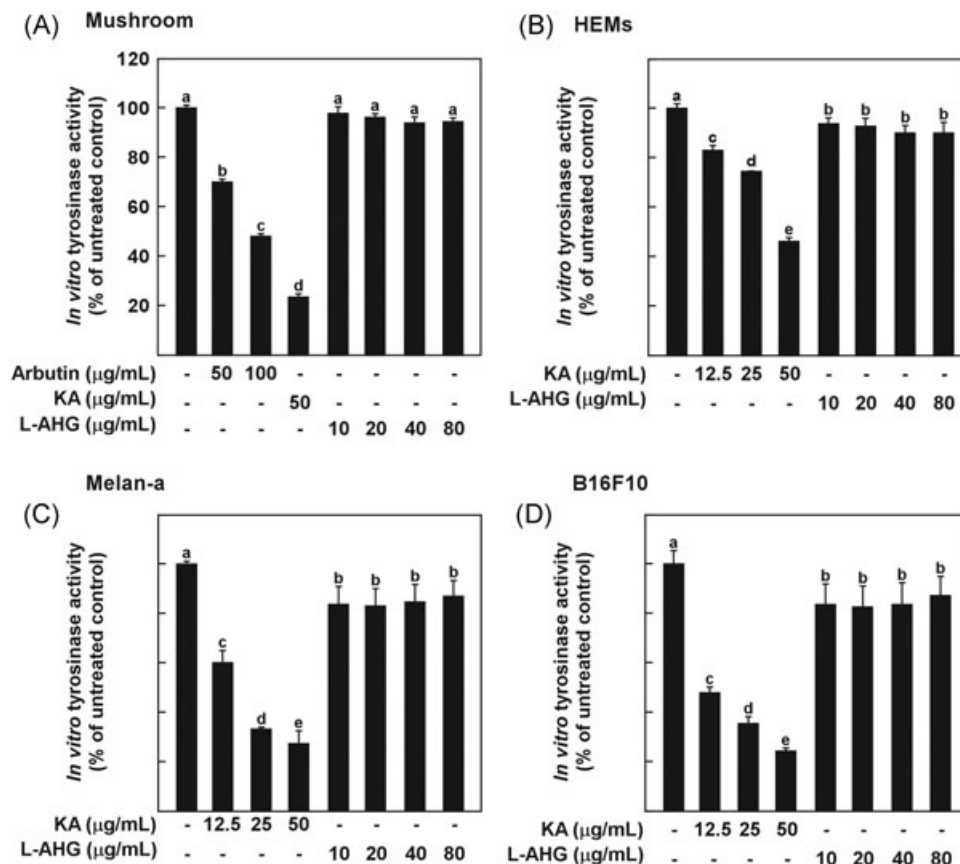

FIGURE 3 Effects of L-AHG on tyrosinase activity in vitro. Effects of L-AHG on in vitro tyrosine hydroxylase activity using (A) mushroom TYR, cell lysates from (B) HEMs, (C) melan-a cells, and (D) B16F10 cells. The tyrosine activity was determined using 1 mM tyrosine as the substrate in the absence and presence of L-AHG. All data (n = 3) represent the mean values ± SD. Means with letters (a-e) in a graph are significantly different from each other at $P < .05$. HEMs, human epidermal melanocytes; L-AHG, 3,6-anhydro-L-galactose; SD, standard deviation; TYR, tyrosinase
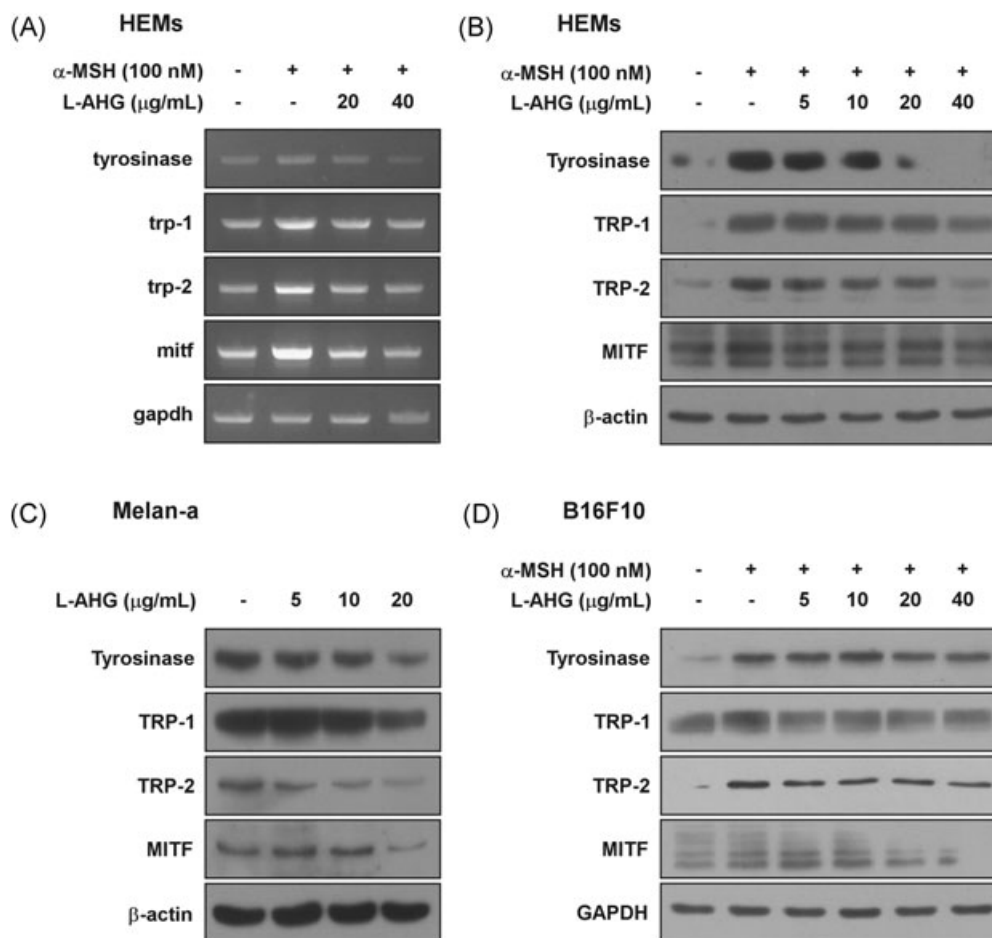
FIGURE 4 Effect of L-AHG on transcriptional and protein levels of melanogenesis-related genes in various melanin-producing cells. (A) Effect of L-AHG on α-MSH-induced transcriptional levels of tyrosinase (TYR), TRP-1, TRP-2, and MITF in HEMs. Cells were pretreated with L-AHG at the indicated concentrations (20 or 40 μg/mL) for 1 hour before being exposed to α-MSH (100 nM) for 1 day. Total RNA were extracted and the mRNA level was measured according to Materials and Methods. (B) Effect of L-AHG on α-MSH-induced protein levels of tyrosinase, TRP-1, TRP-2, and MITF in HEMs. Cells were pretreated with L-AHG at the indicated concentrations for 1 hour before being exposed to α-MSH (100 nM) for 3 days. (C) Effect of L-AHG on protein levels of tyrosinase, TRP-1, TRP-2, and MITF in melan-a cells. Cells were treated with L-AHG at the indicated concentrations (5, 10, or 20 μg/mL) for 3 days. (D) Effect of L-AHG on α-MSH-induced tyrosinase, TRP-1, TRP-2, and MITF in B16F10 cells. Cells were pretreated with L-AHG at the indicated concentrations for 1 hour before being exposed to α-MSH (100 nM) for 3 days. Cell lysates were determined by Western blot analysis as described in Materials and Methods. α-MSH, alpha-melanocyte-stimulating hormone; HEMs, human epidermal melanocytes; L-AHG, 3,6-anhydro-L-galactose; MITF, microphthalmia-associated transcription factor; TRP, tyrosinase related protein

melanogenic enzymes is mediated by MITF, which is a major regulator for melanogenesis and melanocyte-specific genes.[5,6] To investigate whether L-AHG suppresses the expression of melanogenesis genes, reverse transcription-PCR was performed (Figure 4A). L-AHG reduced the transcription of tyrosinase, TRP-1, TRP-2, and MITF in HEMs. Western blot analysis also demonstrated that protein levels of melanogenic proteins were dose dependently decreased by L-AHG treatment (Figure 4B). Moreover, consistent results were observed in murine melanocytes, melan-a cells (Figure 4C), and B1F10 cells (Figure 4D). Taken together, the L-AHG

attenuated melanin production through the downregulation of melanogenesis-related genes.

3.5 | Effect of L-AHG on α-MSH-induced melanogenic melanogenic signal pathways in human melanocytes

Activation of the cAMP/PKA signaling pathway is notably involved in α-MSH-induced melanogenesis and upregulation of melanogenic proteins.[2,8,11] Thus, we examined the effects of L-AHG on the α-MSH-induced cAMP/PKA signaling pathway in HEMs. As shown in
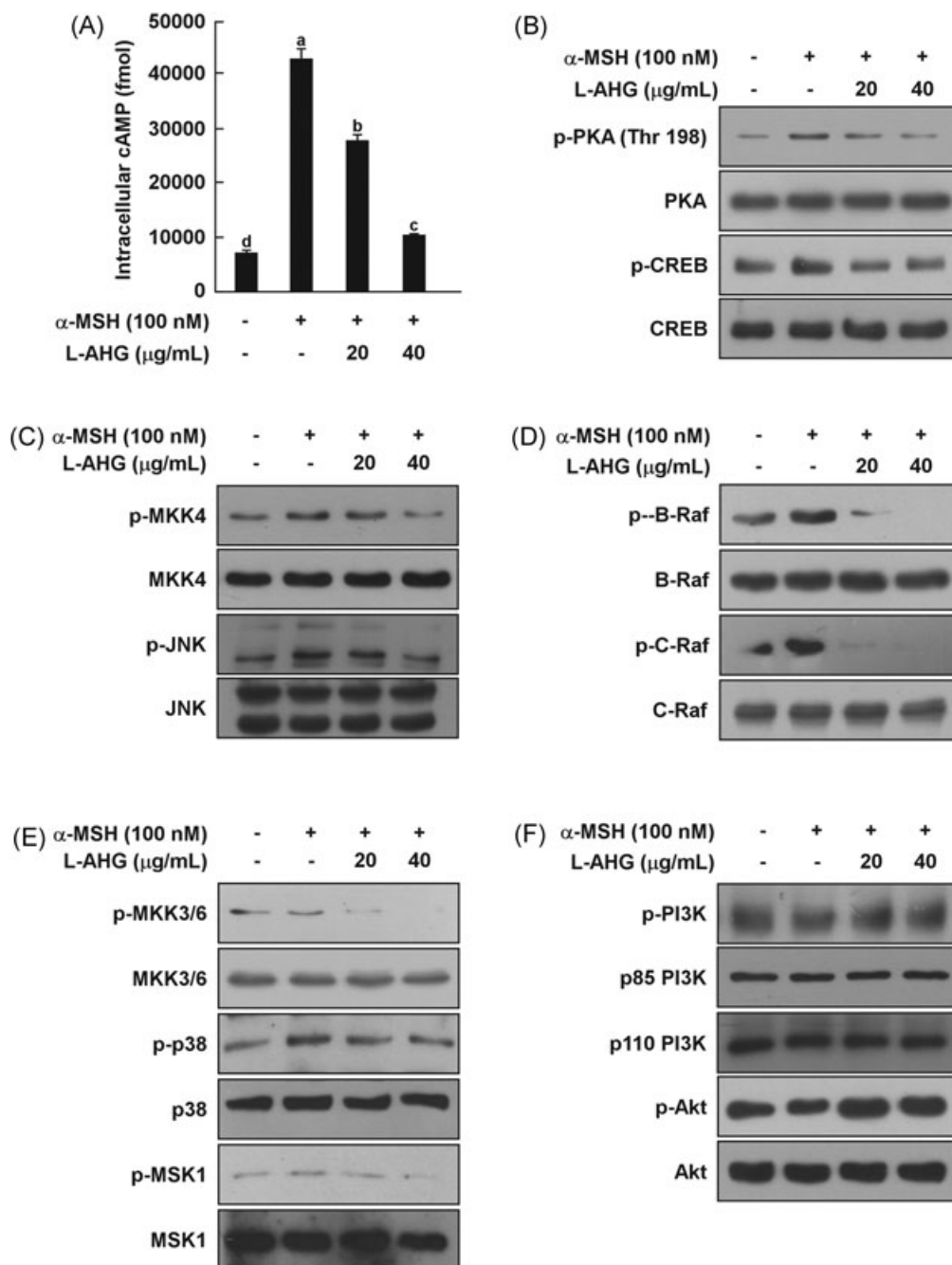
FIGURE 5 Effect of L-AHG on the α-MSH-induced melanogenic signaling pathway in HEMs. L-AHG inhibited α-MSH-induced (A) cAMP levels (B) PKA/CREB, (C) JNK (D) ERK, and (E) p38 signaling in HEMs. Cells were treated with L-AHG (20 or 40 μg/mL) for 1 hour before being exposed to α-MSH (100 nM) and harvested 15 minutes later. (F) L-AHG activated the α-MSH-induced dephosphorylation of Akt signaling. Cells were treated with L-AHG (20 or 40 μg/mL) for 1 hour before being exposed to α-MSH (100 nM) and harvested 30 minutes later. cAMP data (n = 3) represent the mean values ± SD. Means with letters (a-d) in a graph are significantly different from each other at $P < .05$. Western blot analysis was performed using specific antibodies against the respective phosphorylated and total proteins. The data are representative of 3 independent experiments that yielded similar results. α-MSH, alpha-melanocyte-stimulating hormone; cAMP, cyclic adenosine monophosphate; CREB, cAMP response element-binding protein; ERK, extracellular signal-regulated kinase; HEMs, human epidermal melanocytes; JNK, c-Jun N-terminal kinase; L-AHG, 3,6-anhydro-L-galactose; PKA, protein kinase A; SD, standard deviation

Figure 5A, L-AHG attenuated α-MSH-induced cAMP levels in HEMs. Treatment of L-AHG at 40 μg/mL suppressed α-MSH-induced phosphorylation of PKA (Thr198) and CREB (Ser133; Figure 5B). The effect of L-AHG on PKA activity was also indirectly monitored by measuring phosphorylation of the PKA substrate motif (Supporting Information Figure S1).

MAPK signaling pathways, including p38, JNK, and ERK pathways, are known to activate MITF and CREB.[12,13,15,18] L-AHG suppressed the α-MSH-induced phosphorylation of MKK4 and JNK (Figure 5C). Phosphorylation of B-Raf, C-Raf, MEK, ERK, and p90^{RSK} was also decreased by L-AHG treatment in a dose-dependent manner (Figure 5D and Supporting Information Figure S2A). L-AHG also significantly reduced α-MSH-induced phosphorylation of MKK3/6, p38, and MSK1 in HEMs (Figure 5E).

On the other hand, previous studies have reported that MITF expression was negatively regulated by PI3K/Akt signaling.[11,21] L-AHG activated the α-MSH-induced dephosphorylation of PI3K, Akt, mTOR, p70S6K, and GSK3β in HEMs, resulting in MITF downregulation (Figure 5F and Supporting Information Figure S2B). Collectively, these results showed that L-AHG inhibited melanogenic enzyme expression by inactivating cAMP/PKA, MAPK and activating Akt signaling in HEMs.

3.6 | Effect of L-AHG on melanin production in a 3D pigmented human skin model

A 3D human skin-equivalent model is a useful experimental model with morphological and functional characteristics similar to those of in vivo human skin. Therefore, we investigated the effects of L-AHG on melanin production using Neoderm-ME, which is a commercially available 3D pigmented human skin model (Figure 6A). First, the cytotoxic potential of L-AHG was assessed by the MTT assay. No cytotoxicity was observed in the L-AHG treated group compared with phosphate-buffered saline alone (Figure 6B). For the quantification of total melanin, melanin content assays were performed. The total amounts of melanin were reduced, with no dose-dependent effect of L-AHG treatment (Figure 6C). The melanin content in L-AHG-treated groups (25 and 50 μg/mL, 11.9 ± 0.5 and 12.2 ± 0.3 μg/mL, respectively) and arbutin-treated groups (25 μg/mL, 12.8 ± 1.0 μg/mL) was lower than that in the vehicle control group (15.7 ± 0.3 μg/mL). To visualize the melanin in the reconstructed human epidermis model, F/M staining was performed (Figure 6D). We observed a significant decrease in the melanin level in the L-AHG-treated group at 25 μg/mL ($37.5 \pm 8.3\%$) and 50 μg/mL

($37.2 \pm 6.8\%$) compared with phosphate-buffered saline alone ($100\% \pm 7.9$), respectively. Arbutin showed a similar anti-melanogenic effect on the melanin level at 25 μg/mL ($43.2 \pm 5.6\%$). This indicated that the topical application of L-AHG significantly reduced melanin production in the pigmented epidermis model, suggesting similar depigmenting potential in human skin.

4 | DISCUSSION

A number of studies have reported a variety of strategies to develop anti-melanogenic agents that target tyrosinase activity/stability, melanosome maturation/transfer, or melanogenesis-related signaling pathways.[26,27,53] However, several inhibitors directly targeting melanin synthesis have been considered to have insufficient effectiveness and multiple adverse effects.[25,26] Therefore, recently, attention has been focused on an alternative strategy based on melanogenesis-related intracellular signaling pathways.[26,27] Normal skin color is not persistently maintained by intracellular signaling pathways in melanocytes and melanin production is primarily triggered by extrinsic stimuli, such as UV radiation.[27] Therefore, modulators downregulating the activation of melanogenesis to the constitutive level could be new potent anti-melanogenic agents with a low risk of depigmentation in normal skin.[27] Here, we suggest that L-AHG is a novel modulator of melanogenesis-related signaling pathways stimulated by α-MSH. The current study is the first report on the molecular basis of the anti-melanogenic action of L-AHG in human melanocytes and a 3D human skin model.

Treatment of L-AHG did not affect the cell viability of HEMs (Figure 1B). Consistent results were found in other murine cell models, melan-a melanocytes and B16F10 melanoma cells (Figure 1C,D). At noncytotoxic concentrations, L-AHG exerted a significant inhibitory effect on α-MSH-induced melanin synthesis in HEMs (Figure 2A). The same inhibitory effects were also observed in murine melan-a cells (Figure 2B) and B16F10 cells (Figure 2C).

Tyrosinase plays an important role in melanin production by catalyzing L-tyrosine into dopaquinone, followed by melanin pigments.[1] The effect of L-AHG on tyrosinase activity was examined using L-tyrosine as a substrate. Purified mushroom tyrosinase and cell lysates extracted from each cell models were used for an in vitro tyrosinase activity assay. L-AHG did not inhibit both mushroom and cellular tyrosinase oxidative activity up to 80 μg/mL (Figure 3). These results suggest that L-AHG exerted anti-melanogenic activity, but did not directly target tyrosinase activity, suggesting another mechanism of action.
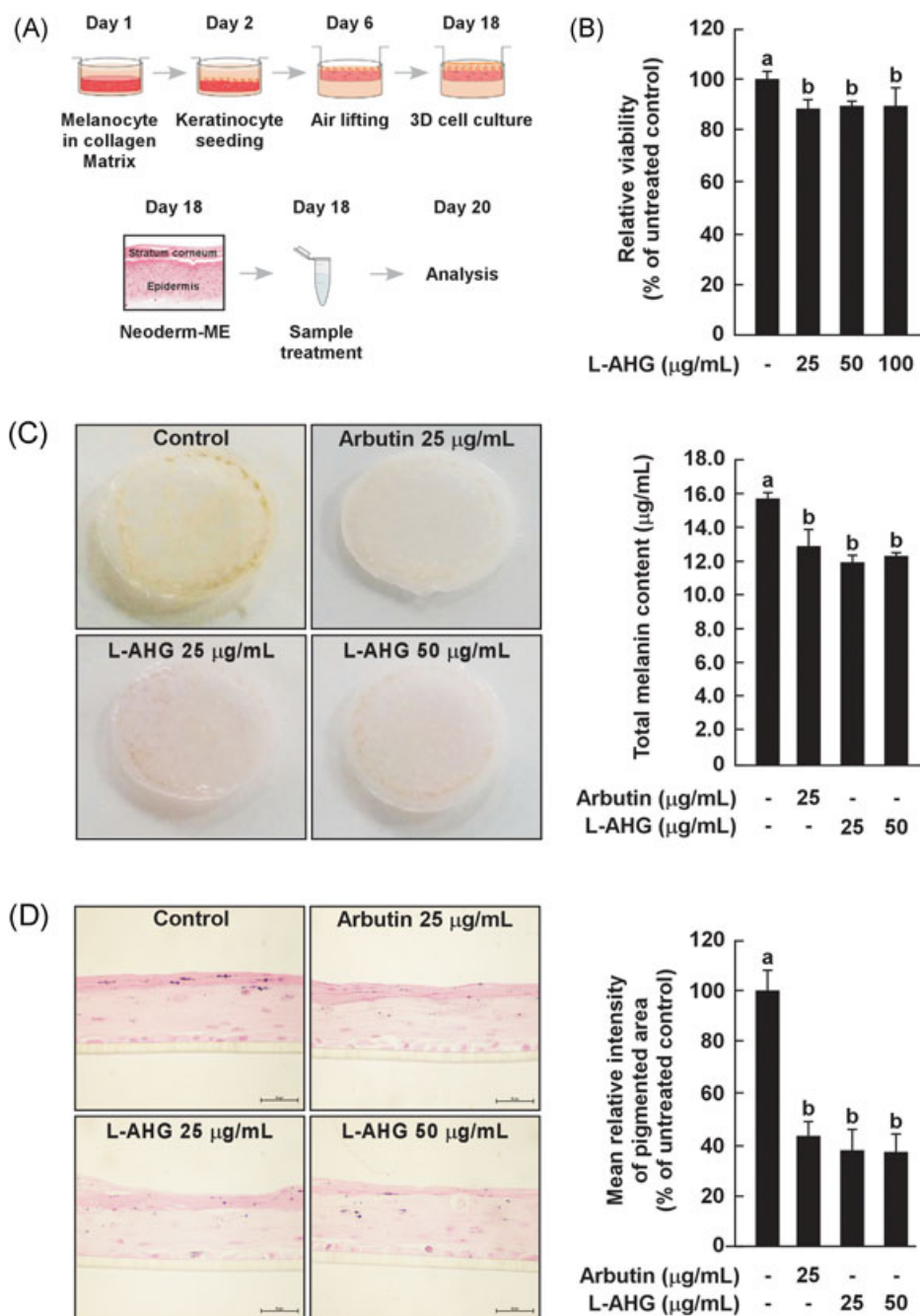
FIGURE 6 Effects of L-AHG in a 3D pigmented human skin model. (A) A schematic diagram of a 3D human skin culture system. The figure was adapted from a previous study and modified slightly.[58] (B) Effect of L-AHG on tissue viability in a 3D human epidermis model. L-AHG was treated at the indicated concentrations (0, 25, 50, 100 μg/mL) for 2 days. All data (n = 3) represent the mean values ± SD. (C) Effects of L-AHG on the total melanin content in a 3D pigmented human skin model. The total amounts of melanin were analyzed by the melanin content assay. (D) Fontana-Masson staining was performed as described in the Materials and Methods. All cells were photographed under equal magnification using an inverted phase-contrast microscope. Data are representative of 2 independent experiments that yielded similar results. The mean relative intensity of the pigmented area was analyzed using Image J program. All data (n = 2) represent the mean values ± SD. Means with letters (a,b) in a graph are significantly different from each other at $P < .05$. 3D, 3 dimensional; L-AHG, 3,6-anhydro-L-galactose; SD, standard deviation

Upregulation of melanogenic proteins, including tyrosinase, TRP-1, TRP-2, and transcription factor MITF, promotes melanin synthesis by various stimuli, such as α-MSH and UV.[1,8,9] Reverse transcription-PCR and Western blot analysis displayed that L-AHG reduced α-MSH-induced transcriptional and protein levels of tyrosinase, TRP-1, TRP-2, and MITF in HEMs (Figure 4A,B). Protein levels of melanogenic proteins
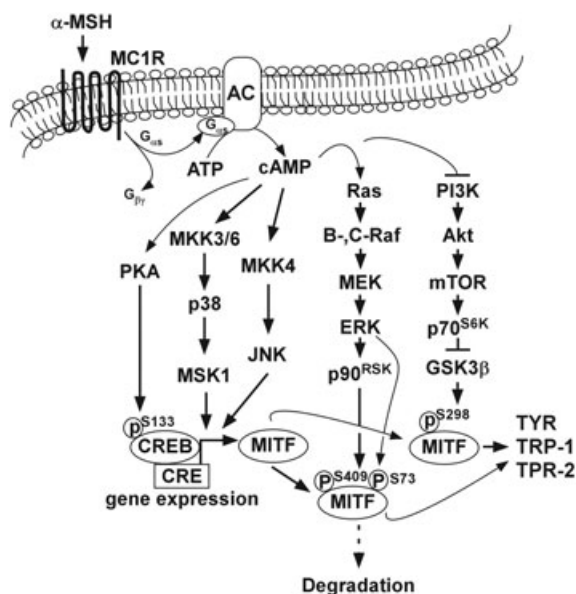
FIGURE 7 Proposed molecular mechanism of melanogenesis stimulated by α-MSH. L-AHG inhibits α-MSH-induced melanogenesis by regulating the cAMP/PKA, MAPK, and Akt signaling pathways. α-MSH, alpha-melanocyte-stimulating hormone; cAMP, cyclic adenosine monophosphate; L-AHG, 3,6-anhydro-L-galactose; MAPK, mitogen-activated protein kinase; PKA, protein kinase A

were dose dependently decreased by L-AHG treatment in murine cell models (Figure 4C,D). Collectively, the L-AHG decreased α-MSH-induced melanin production through the downregulation of melanogenesis-related genes.

To understand the mechanism underlying the anti-melanogenic effect of L-AHG, melanogenesis-related signal pathways were determined by Western blot analysis. α-MSH-induced melanogenesis is related to various signaling pathways, including cAMP/PKA, MAPK, and Akt pathways.[9,10] Stimulation of MC1R by α-MSH triggers intracellular cAMP production, followed by the activation of PKA and MAPK, including JNK, ERK, and the p38 signal pathway.[15,16,18,45,54] In human melanocytes, activation of cAMP/PKA and MAPK signal pathways upregulates phosphorylation of CREB and expression of MITF, tyrosinase, and TRPs, leading to melanogenesis.[4,7] L-AHG downregulated α-MSH-induced transcriptional levels of melanogenesis-related genes by inhibiting PKA (Figure 5A,B) and the MAPK signaling pathway (Figure 5C-E). Meanwhile, it has been suggested that an increased level of cAMP results in phosphorylation and activation of MITF via inhibition of PI3K/Akt/mTOR/p70S6K/GSK3β in melanocytes and melanoma cells.[20-23] Consequently, activation of GSK3β facilitates MITF binding to the M box of the tyrosinase promoter, thereby resulting in the transcriptional stimulation of tyrosinase gene.[16,24] L-AHG recovered

α-MSH-induced dephosphorylation of the PI3K/Akt signal pathway (Figure 5F). Collectively, L-AHG attenuated α-MSH-melanin production by interrupting the cAMP/PKA, MAPK, and Akt signal pathways in human melanocytes (Figure 7).

A 3D pigmented reconstructed skin model is experimental models designed to mimic the morphology and physiology of human skin.[25,55] A 3D pigmented skin model has been used as a preclinical model to screen the efficacy of melanogenesis regulators.[25,55] In addition, a reconstructed human skin model has been shown to have properties similar to those of in vivo UV-induced pigmentation.[25,56] To evaluate the anti-melanogenic effect of L-AHG under in vivo conditions, Neoderm®-ME was used, which is a commercially available model of pigmented human epidermis.[25,57] The cytotoxic potential of L-AHG was assessed in a human epidermis model using the MTT assay (Figure 6B). L-AHG did not affect the tissue viability up to 100 μg/mL (approximately 90% of control). This result indicated that the anti-melanogenic effect of L-AHG was not a result of cytotoxicity. The total melanin content assay and F/M staining showed that topical application of L-AHG significantly reduced the melanin level in the 3D pigmented epidermis model similar to arbutin (Figure 6C,D). Unexpectedly, L-AHG treatment did not show a dose-dependent anti-melanogenic capacity in a 3D human model. These phenomena may be attributed to the chemical characteristic of L-AHG. L-AHG may possess limited skin-absorption ability to penetrate skin layers because L-AHG is a hydrophilic sugar. To clarify this, further studies are required to elucidate the bioavailability and penetration ability of L-AHG in a human skin model.

In conclusion, L-AHG, the most abundant and bioactive sugar of agarose, exhibited significant inhibitory activity on α-MSH-induced melanogenesis in human and murine melanocytes. Although L-AHG did not inhibit tyrosinase activity in vitro, it dose dependently suppressed the α-MSH-induced expression of melanogenic enzymes in human and murine melanocytes. This inhibition is mediated primarily by disruption of the cAMP/PKA, MAPK, and Akt signaling pathway and the subsequent downregulation of transcription factor MITF expression. Topical application of L-AHG significantly reduced the total melanin level in the 3D pigmented epidermis model. Considering these results together, we provide insight into the biological actions of L-AHG and the molecular basis for the development of a new skin-whitening agent.

ACKNOWLEDGMENTS

prepared at the Korea University Food Safety Hall for the Institute of Biomedical Science and Food Safety.

CONFLICTS OF INTEREST

The authors declare no conflicts of interest.

ORCID

Nam Joo Kang http://orcid.org/0000-0003-1500-2845

REFERENCES

1. Videira IFS, Moura DFL, Magina S. Mechanisms regulating melanogenesis. *An Bras Dermatol.* 2013;88:76-83.
2. Costin GE, Hearing VJ. Human skin pigmentation: melanocytes modulate skin color in response to stress. *FASEB J.* 2007;21:976-994.
3. Briganti S, Camera E, Picardo M. Chemical and instrumental approaches to treat hyperpigmentation. *Pigment Cell Res.* 2003;16:101-110.
4. Gillbro JM, Olsson MJ. The melanogenesis and mechanisms of skin-lightening agents—existing and new approaches. *Int J Cosmet Sci.* 2011;33:210-221.
5. Solano F, Briganti S, Picardo M, Ghanem G. Hypopigmenting agents: an updated review on biological, chemical and clinical aspects. *Pigment Cell Res.* 2006;19:550-571.
6. Yamaguchi Y, Hearing VJ. Physiological factors that regulate skin pigmentation. *Biofactors.* 2009;35:193-199.
7. Busca R, Ballotti R. Cyclic AMP a key messenger in the regulation of skin pigmentation. *Pigment Cell Res.* 2000;13:60-69.
8. Park HY, Kosmadaki M, Yaar M, Gilchrest BA. Cellular mechanisms regulating human melanogenesis. *Cell Mol Life Sci.* 2009;66:1493-1506.
9. D'mello S, Finlay G, Baguley B, Askarian-Amiri M. Signaling pathways in melanogenesis. *Int J Mol Sci.* 2016;17:E1144.
10. Rodriguez CI, Setaluri V. Cyclic AMP (cAMP) signaling in melanocytes and melanoma. *Arch Biochem Biophys.* 2014;563:22-27.
11. Roh E, Yun CY, Young Yun J, et al. cAMP-binding site of PKA as a molecular target of bisabolangelone against melanocyte-specific hyperpigmented disorder. *J Invest Dermatol.* 2013;133:1072-1079.
12. Gu WJ, Ma HJ, Zhao G, et al. Additive effect of heat on the UVB-induced tyrosinase activation and melanogenesis via ERK/p38/MITF pathway in human epidermal melanocytes. *Arch Dermatol Res.* 2014;306:583-590.
13. Newton RA, Roberts DW, Leonard JH, Sturm RA. Human melanocytes expressing MC1R variant alleles show impaired activation of multiple signaling pathways. *Peptides.* 2007;28:2387-2396.
14. Bellei B, Maresca V, Flori E, Pitisci A, Larue L, Picardo M. p38 regulates pigmentation via proteasomal degradation of tyrosinase. *J Biol Chem.* 2010;285:7288-7299.
15. Herraiz C, Journé F, Abdel-Malek Z, Ghanem G, Jiménez-Cervantes C, García-Borrón JC. Signaling from the human melanocortin 1 receptor to ERK1 and ERK2 mitogen-activated protein kinases involves transactivation of cKIT. *Mol Endocrinol.* 2011;25:138-156.
16. Khaled M, Larribere L, Bille K, et al. Glycogen synthase kinase 3β is activated by cAMP and plays an active role in the regulation of melanogenesis. *J Biol Chem.* 2002;277:33690-33697.
17. Lee CH, Kim HT, Yun EJ, et al. A novel agarolytic β-galactosidase acts on agarooligosaccharides for complete hydrolysis of agarose into monomers. *Appl Environ Microbiol.* 2014;80:5965-5973.
18. Tada A, Pereira E, Beitner-Johnson D, Kavanagh R, Abdel-Malek ZA. Mitogen- and ultraviolet-B-induced signaling pathways in normal human melanocytes. *J Invest Dermatol.* 2002;118:316-322.
19. Jin ML, Park SY, Kim YH, Park G, Son HJ, Lee SJ. Suppression of alpha-MSH and IBMX-induced melanogenesis by cordycepin via inhibition of CREB and MITF, and activation of PI3K/Akt and ERK-dependent mechanisms. *Int J Mol Med.* 2011;29:119-124.
20. Bellei B, Flori E, Izzo E, Maresca V, Picardo M. GSK3β inhibition promotes melanogenesis in mouse B16 melanoma cells and normal human melanocytes. *Cell Signal.* 2008;20:1750-1761.
21. Tu CX, Lin M, Lu SS, Qi XY, Zhang RX, Zhang YY. Curcumin inhibits melanogenesis in human melanocytes. *Phytother Res.* 2012;26:174-179.
22. Ohguchi K, Banno Y, Nakagawa Y, Akao Y, Nozawa Y. Negative regulation of melanogenesis by phospholipase D1 through mTOR/p70 S6 kinase 1 signaling in mouse B16 melanoma cells. *J Cell Physiol.* 2005;205:444-451.
23. Tachibana M. Cochlear melanocytes and MITF signaling. *J Investig Dermatol Symp Proc.* 2001;6:95-98.
24. Yasumoto K, Yokoyama K, Takahashi K, Tomita Y, Shibahara S. Functional analysis of microphthalmia-associated transcription factor in pigment cell-specific transcription of the human tyrosinase family genes. *J Biol Chem.* 1997;272:503-509.
25. Gunia-Krzyżak A, Popiol J, Marona H. Melanogenesis inhibitors: strategies for searching for and evaluation of active compounds. *Curr Med Chem.* 2016;23:3548-3574.
26. Bin BH, Kim S, Bhin J, Lee T, Cho EG. The development of sugar-based anti-melanogenic agents. *Int J Mol Sci.* 2016;17:583.
27. Imokawa G, Ishida K. Inhibitors of intracellular signaling pathways that lead to stimulated epidermal pigmentation: perspective of anti-pigmenting agents. *Int J Mol Sci.* 2014;15:8293-8315.
28. Ahmed ABA, Adel M, Karimi P, Peidayesh M. Pharmaceutical, cosmeceutical, and traditional applications of marine carbohydrates. *Adv Food Nutr Res.* 2014;73:197-220.
29. Cha SH, Ko SC, Kim D, Jeon YJ. Screening of marine algae for potential tyrosinase inhibitor: those inhibitors reduced tyrosinase activity and melanin synthesis in zebrafish. *J Dermatol.* 2011;38:343-352.
30. Thomas N, Kim SK. Beneficial effects of marine algal compounds in cosmeceuticals. *Mar Drugs.* 2013;11:146-164.
31. Laurienzo P. Marine polysaccharides in pharmaceutical applications: an overview. *Mar Drugs.* 2010;8:2435-2465.
32. Kim J, Yun E, Yu S, Kim K, Kang N. Different levels of skin whitening activity among 3,6-anhydro-L-galactose,

agarooligosaccharides, and neoagarooligosaccharides. *Mar Drugs*. 2017;15:E321.

33. Yun EJ, Choi IG, Kim KH. Red macroalgae as a sustainable resource for bio-based products. *Trends Biotechnol*. 2015; 33:247-249.

34. Yun EJ, Lee S, Kim JH, et al. Enzymatic production of 3,6-anhydro-L-galactose from agarose and its purification and in vitro skin whitening and anti-inflammatory activities. *Appl Microbiol Biotechnol*. 2013;97:2961-2970.

35. Kim JH, Yun EJ, Seo N, et al. Enzymatic liquefaction of agarose above the sol–gel transition temperature using a thermostable endo-type β-agarase, Aga16B. *Appl Microbiol Biotechnol*. 2017;101:1111-1120.

36. Kim K, Leutou AS, Jeong H, et al. Anti-pigmentary effect of (-)-4-hydroxysattabacin from the marine-derived *Bacterium Bacillus* sp. *Mar Drugs*. 2017;15:E138.

37. Sugano Y, Kodama H, Terada I, Yamazaki Y, Noma M. Purification and characterizaion of a novel enzyme, α-neoagarooligosaccharide hydrolase (α-NAOS hydrolase), from a marine bacterium, Vibrio sp. strain JT0107. *J Bacteriol*. 1994;176:6812-6818.

38. Miller I, Wong H, Newman R. A [13]C N.M.R. study of some disaccharides from algal polysaccharides. *Aust J Chem*. 1982;35:853-856.

39. Araki C, Hirase S. Studies on the chemical constitution of agar-agar. XV. Exhaustive mercaptolyses of agar-agar. *Bull Chem Soc Jpn*. 1953;26:463-467.

40. Mayer TC, Oddis L. Pigment cell differentiation in embryonic mouse skin and isolated epidermis: an *in vitro* study. *J Exp Zool*. 1977;202:415-424.

41. Bennett DC, Cooper PJ, Hart IR. A line of non-tumorigenic mouse melanocytes, syngeneic with the B16 melanoma and requiring a tumour promoter for growth. *Int J Cancer*. 1987;39:414-418.

42. An SM, Koh JS, Boo YC. p-coumaric acid not only inhibits human tyrosinase activity in vitro but also melanogenesis in cells exposed to UVB. *Phytother Res*. 2010;24:1175-1180.

43. Friedmann PS, Gilchrest BA. Ultraviolet radiation directly induces pigment production by cultured human melanocytes. *J Cell Physiol*. 1987;133:88-94.

44. Gordon PR, Mansur CP, Gilchrest BA. Regulation of human melanocyte growth, dendricity, and melanization by keratinocyte derived factors. *J Invest Dermatol*. 1989;92:565-572.

45. Lee CS, Jang WH, Park M, et al. A novel adamantyl benzylbenzamide derivative, AP736, suppresses melanogenesis through the inhibition of cAMP-PKA-CREB-activated microphthalmia-associated transcription factor and tyrosinase expression. *Exp Dermatol*. 2013;22:762-764.

46. Commo S, Gaillard O, Thibaut S, Bernard BA. Absence of TRP-2 in melanogenic melanocytes of human hair. *Pigment Cell Res*. 2004;17:488-497.

47. Klabunde T, Eicken C, Sacchettini JC, Krebs B. Crystal structure of a plant catechol oxidase containing a dicopper center. *Nat Struct Biol*. 1998;5:1084-1090.

48. Kwon BS, Haq AK, Pomerantz SH, Halaban R. Isolation and sequence of a cDNA clone for human tyrosinase that maps at the mouse c-albino locus. *Proc Natl Acad Sci USA*. 1987;84:7473-7477.

49. Lerch K. Amino acid sequence of tyrosinase from *Neurospora crassa*. *Proc Natl Acad Sci USA*. 1978;75:3635-3639.

50. Funayama M, Arakawa H, Yamamoto R, Nishino T, Shin T, Murao S. Effects of alpha- and beta-arbutin on activity of tyrosinases from mushroom and mouse melanoma. *Biosci Biotechnol Biochem*. 1995;59:143-144.

51. Galindo JD, Martinez JH, Lopez-Ballester JA, Peñafiel R, Solano F, Lozano JA. The effect of polyamines on tyrosinase activity. *Biochem Int*. 1987;15:1151-1158.

52. Jacobsohn GM, Jacobsohn MK. Incorporation and binding of estrogens into melanin: comparison of mushroom and mammalian tyrosinases. *Biochim Biophys Acta*. 1992;1116:173-182.

53. Ando H, Kondoh H, Ichihashi M, Hearing VJ. Approaches to identify inhibitors of melanin biosynthesis via the quality control of tyrosinase. *J Invest Dermatol*. 2007;127:751-761.

54. Lee CS, Park M, Han J, et al. Liver X receptor activation inhibits melanogenesis through the acceleration of ERK-mediated MITF degradation. *J Invest Dermatol*. 2013;133: 1063-1071.

55. Yoon TJ, Lei TC, Yamaguchi Y, Batzer J, Wolber R, Hearing VJ. Reconstituted 3-dimensional human skin of various ethnic origins as an in vitro model for studies of pigmentation. *Anal Biochem*. 2003;318:260-269.

56. Duval C, Regnier M, Schmidt R. Distinct melanogenic response of human melanocytes in mono-culture, in co-culture with keratinocytes and in reconstructed epidermis, to UV exposure. *Pigment Cell Res*. 2001;14:348-355.

57. Lee M, Park H, Jeon SW, et al. Novel anti-melanogenic hexapeptoids, PAL-10 and PAL-12. *Arch Dermatol Res*. 2015;307:249-257.

58. Park G, Baek S, Kim JE, et al. Flt3 is a target of coumestrol in protecting against UVB-induced skin photoaging. *Biochem Pharmacol*. 2015;98:473-483.

SUPPORTING INFORMATION

Additional supporting information may be found online in the Supporting Information section at the end of the article.